Essential oil extract p-cresol effect on Ca^{2+} signaling and its underlying mechanism in DBTRG-05MG human glioblastoma cells

PIN-HAO CHOU[1,2,*], CHUN-LANG SU[3,4,*], SHIH-HAU FU[1], ROBERT SCHLEIP[5] and WEI-ZHE LIANG[6,7]

[1]Department of Acupressure Technology, Chung Hwa University of Medical Technology, Tainan 717302, Taiwan, R.O.C.; [2]Stark Works Co., Ltd. Taipei 10491, Taiwan, R.O.C.; [3]Chung Jen Junior College of Nursing, Health Science and Management, Chiayi 60077, Taiwan, R.O.C.; [4]Department of Rehabilitation, Tung Wah Hospital, Nantou 557, Taiwan, R.O.C.; [5]European Rolfing Association, Medical Faculty of Ulm University, D-89081 Ulm, Germany; [6]Department of Pharmacy and Master Program, College of Pharmacy and Health Care, Tajen University, Yanpu, Pingtung 907101, Taiwan, R.O.C.; [7]Department of Medical Education and Research, Kaohsiung Veterans General Hospital, Kaohsiung 813414, Taiwan, R.O.C.

Received May 17, 2024; Accepted July 5, 2024

DOI: 10.3892/br.2025.1958

Abstract. The effect of para (p)-cresol, an essential oil component, on calcium ion (Ca^{2+}) signaling in human glioblastoma is unknown. The present study aimed to investigate how p-cresol influences intracellular Ca^{2+} levels ($[Ca^{2+}]_i$) and viability in DBTRG-05MG human glioblastoma cells. Cells were treated with p-cresol to assess its impact on cell viability and $[Ca^{2+}]_i$. Cell viability was evaluated using a WST-1 assay. $[Ca^{2+}]_i$ was measured using a fluorescence-based Ca^{2+} indicator. Cells were loaded with the Ca^{2+}-sensitive dye (fura-2), and fluorescence intensity was recorded before and after p-cresol treatment to determine changes in $[Ca^{2+}]_i$. p-Cresol induced concentration-dependent increases in $[Ca^{2+}]_i$ between 50 and 150 μM. At 50-250 μM, p-cresol triggered cell death; this effect was reversed by pretreating the cells with the Ca^{2+} chelator BAPTA-AM. The removal of extracellular Ca^{2+} inhibited Ca^{2+} entry. p-Cresol-induced Ca^{2+} influx was confirmed by Mn^{2+}-induced quenching of fura-2 fluorescence. Store-operated Ca^{2+} channel modulators SKF96365 and 2-aminoethoxydiphenyl borate and the protein kinase C inhibitor GF109203X inhibited p-cresol-induced Ca^{2+} entry, but voltage-gated Ca^{2+} channel blocker nifedipine did not. Treatment with the endoplasmic reticulum Ca^{2+} pump inhibitor thapsigargin in Ca^{2+}-free medium inhibited p-cresol-induced $[Ca^{2+}]_i$ rises; conversely, treatment with p-cresol decreased thapsigargin-induced $[Ca^{2+}]_i$ rises. Furthermore, phospholipase C (PLC) inhibition with U73122 abolished p-cresol-induced $[Ca^{2+}]_i$ rises. In DBTRG-05MG cells, p-cresol triggered Ca^{2+}-associated cell death. The process involved the entry of Ca^{2+} through PKC-regulated store-operated Ca^{2+} channels and release of Ca^{2+} from the endoplasmic reticulum, which depends on PLC. Additionally, BAPTA-AM, which has Ca^{2+}-chelating properties, may be a promising compound in preventing p-cresol-induced cytotoxicity, a potential breakthrough in neurotoxic research in glioblastoma cell model.

Introduction

Cresols are organic compounds, also known as methylphenols, which have various biological effects: Dinitro-o-cresol induces cell death but does not change oxidase expression in soybean cells (1) and causes cytotoxicity via apoptosis in LNCaP prostate cancer cells (2). Additionally, 3-methyl-4-nitrophenol induces toxic effects in rat renal tubular epithelial cells (3). Para (p)-cresol is found in various essential oils from plants such as cloves, cinnamon and basil, contributing to their unique scent (4,5). p-Cresol has been shown to affect proliferation, viability, differentiation and glucose uptake in 3T3-L1 adipocytes (6) and induce cytotoxicity in polymorphonuclear cells (7). Furthermore, p-cresol is rapidly absorbed and excreted, primarily into urine as conjugate metabolites in rats (8). However, it is still unclear how p-cresol affects physiology in human glioblastoma.

Changes in concentration of calcium ions (Ca^{2+}) inside cells, known as intracellular Ca^{2+} concentration ($[Ca^{2+}]_i$), play a crucial role in regulating various cell processes associated with cell death (9,10). Cells use several mechanisms to regulate $[Ca^{2+}]_i$ both globally and at the subcellular level. One of the mechanisms involves G-protein-coupled receptors, which activate phospholipase C (PLC) to release Ca^{2+} from

Correspondence to: Dr Wei-Zhe Liang, Department of Pharmacy and Master Program, College of Pharmacy and Health Care, Tajen University, 20 Weixin Road, Yanpu, Pingtung 907101, Taiwan, R.O.C
E-mail: lianggoole67@gmail.com

*Contributed equally

Key words: p-cresol, human glioblastoma cell, Ca^{2+} signaling, store-operated Ca^{2+} channel, endoplasmic reticulum

intracellular stores and influence Ca^{2+} entry across the plasma membrane (9,10). Understanding the mechanisms underlying compound-induced increases in intracellular Ca^{2+} is crucial to comprehend the biological effects on the cell.

To the best of our knowledge, there is a scarcity of literature that discusses the effect of cresol-related compounds in Ca^{2+} signaling. 4-chloro-m-cresol is the most studied cresol and is commonly used as an inhibitor of sarcoendoplasmic reticulum calcium ATPase Ca^{2+} pumps (11,12). Non-specific effects of 4-chloro-m-cresol may cause Ca^{2+} flux and respiratory burst in human neutrophils (13). Additionally, 4-chloro-m-cresol increases myoplasmic free Ca^{2+} concentration and force of contraction in mouse skeletal muscle (14) and inhibits voltage-gated potassium (K^+) channels at the rat calyx of Held (15). Since p-cresol has a similar structure to 4-chloro-m-cresol, p-cresol may affect Ca^{2+} homeostasis in cell models.

p-Cresol has been implicated in various pathological conditions due to its cytotoxic effects on different cell types, such as 3T3-L1 adipocytes (6) and polymorphonuclear cells (7). To the best of our knowledge, however, no studies have examined its impact on the cytotoxicity in human glioma cells. Glioma, particularly glioblastoma multiforme (GBM), is known for its aggressive nature and poor prognosis (16-18). The 5-year survival rate for GBM is less than 10%, with a median survival time of approximately 15 months following diagnosis (16-18). The incidence of GBM varies by region, but it is generally reported at 3-4 cases/100,000 individuals annually (16-18). This data highlights the urgent need for effective therapeutic strategies to improve outcomes for patients. Understanding the molecular and cellular mechanisms underlying glioma pathophysiology has driven extensive research (16-18). Exploring environmental and metabolic factors influencing glioma progression is key for identifying novel therapeutic targets.

Understanding how p-cresol influences glioma cell biology may reveal novel insights into the environmental factors contributing to glioma progression, as well as potential biomarkers for glioma prognosis and therapeutic targets. Prevalence of glioma has gradually increased, with current incidence rates reported at ~6 cases per 100,000 individuals annually in North America and Europe over the past decade (16-18). Despite advancements in surgical techniques, radiation therapy and chemotherapy, the overall efficacy of current treatment options remains limited, particularly for aggressive forms such as GBM (16-18). Given these challenges, exploring novel therapeutic avenues, including the impact of essential oil components such as p-cresol, could have practical applications in improving glioma treatment outcomes. This may contribute to developing more effective strategies for managing glioma progression and improving patient outcomes.

Ca^{2+} signaling serves a key role in various cellular processes, including proliferation, migration and apoptosis. Because these processes contribute to tumor growth, invasion, and resistance to treatment, they are particularly relevant in cancer biology (9,10). In glioblastoma, dysregulated Ca^{2+} signaling is implicated in tumor progression and resistance to therapy. Elevated intracellular Ca^{2+} levels activate various downstream pathways, leading to changes in gene expression, metabolic activity and cell behavior (9,10). PLC is a key enzyme in the Ca^{2+} signaling pathway, catalyzing hydrolysis of phosphatidylinositol 4,5-bisphosphate (PIP_2) to generate inositol 1,4,5-trisphosphate (IP_3) and diacylglycerol (DAG). IP_3 binds to its receptors on the endoplasmic reticulum, leading to release of Ca^{2+} into the cytoplasm. When agonists activate cells, PLC is stimulated, leading to the breakdown of PIP_2 into IP_3 and DAG (9). Increased DAG concentration activates protein kinase C (PKC), while IP_3 binds IP_3 receptor in the endoplasmic reticulum, causing Ca^{2+} release from internal stores (9). This increase in $[Ca^{2+}]_i$ triggers downstream signaling pathways that contribute to glioblastoma cell survival and proliferation (9,10). Understanding the specific roles of PLC isoforms in Ca^{2+} signaling may reveal novel therapeutic targets for glioblastoma. Targeting dysregulated PLC-mediated pathways may enhance the efficacy of existing treatments or lead to the development of novel therapeutic strategies (9,10).

Although p-cresol has been shown to promote blood-brain barrier (BBB) integrity and cross BBB *in vivo* (19), it is unknown how p-cresol affects $[Ca^{2+}]_i$ in human glioblastoma. The present study aimed to investigate this effect using DBTRG-05MG human glioblastoma cells, a commonly used model for glioblastoma research (20-22). Fluorescent Ca^{2+}-sensitive dye fura-2-AMwas used to measure changes in $[Ca^{2+}]_i$ in response to p-cresol. Additionally, the study explored the effect of p-cresol on cell viability.

Materials and methods

Chemicals. p-Cresol (Fig. 1A), WST-1, nifedipine (voltage-gated Ca^{2+} channel blocker), SKF96365 (store-operated Ca^{2+} entry modulator), GF109203X (a PKC inhibitor), thapsigargin (an inhibitor of the endoplasmic reticulum Ca^{2+} pump), ATP, and U73122 (a PLC inhibitor) were obtained from Sigma-Aldrich (Merck KGaA). Fura-2-AM, 1,2-bis(2-aminophenoxy)ethane-N,N,N'N'-tetraacetic acid (BAPTA-AM), and 2-aminoethoxydiphenyl borate (2-APB) were obtained from Molecular Probes. Finally, the reagents for cell culture, including RPMI-1640 medium, fetal bovine serum (FBS), penicillin, and streptomycin, were obtained from Gibco (Thermo Fisher Scientific, Inc.).

Cell culture. DBTRG-05MG human glioblastoma cells from Bioresource Collection and Research Center (Taiwan) were cultured in RPMI-1640 medium with 10% heat-inactivated FBS, 100 U/ml penicillin, and 100 μg/ml streptomycin, all obtained from Gibco (Thermo Fisher Scientific, Inc.), at 37˚C in a humidified atmosphere containing 5% carbon dioxide (CO_2).

Solutions used in $[Ca^{2+}]_i$ measurements. The Ca^{2+}-containing medium at pH 7.4 contained the following components and concentrations: NaCl (140 mM), KCl (5 mM), $MgCl_2$ (1 mM), $CaCl_2$ (2 mM), HEPES (10 mM), and glucose (10 mM). The Ca^{2+}-free medium had the same components, with $CaCl_2$ replaced by 2 mM EGTA. p-Cresol was dissolved in ethanol to make a 0.1 M stock solution. Other chemicals were dissolved in water, ethanol or DMSO. The impact of organic solvent concentration (≤0.1%) on cell viability and basal $[Ca^{2+}]_i$ was determined through control experiments. Cells were exposed

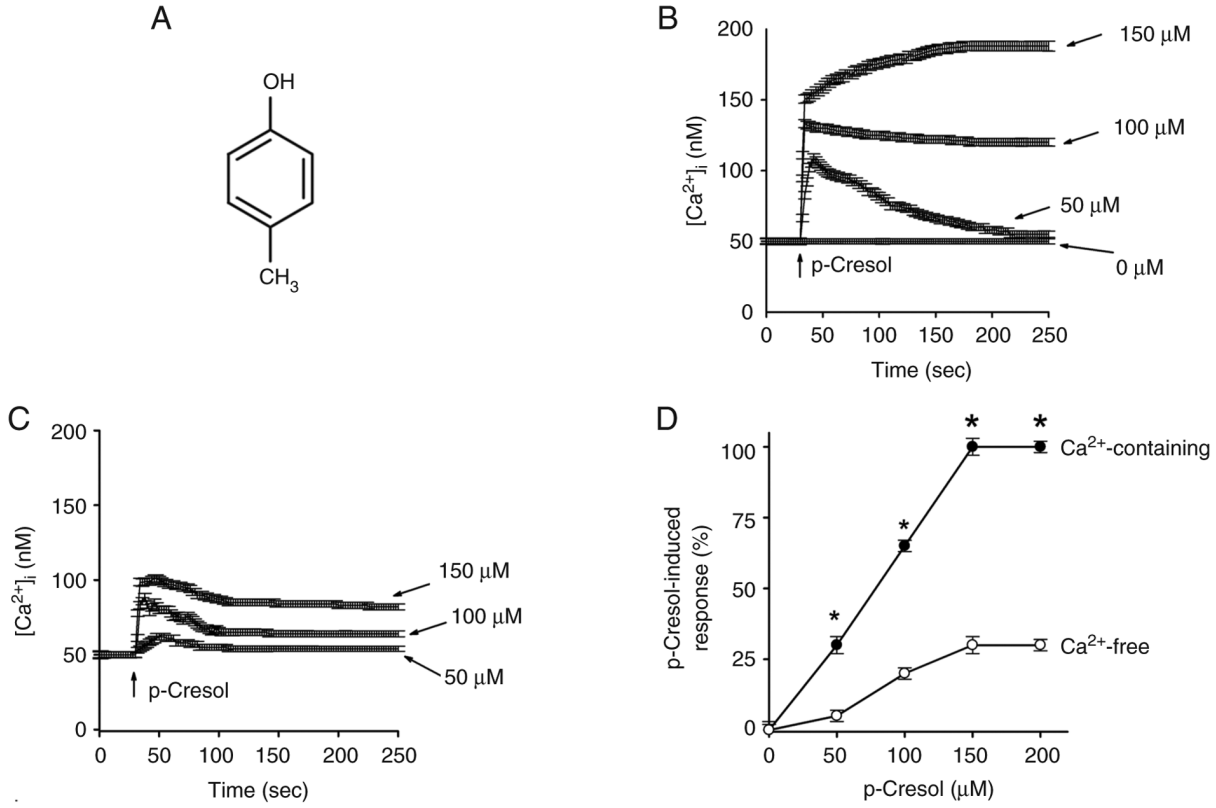

Figure 1. Effect of p-cresol on $[Ca^{2+}]_i$. (A) Structure of p-cresol. p-cresol was added in Ca^{2+} (B) -containing and (C) -free medium. (D) Concentration-response plots of p-cresol-induced $[Ca^{2+}]_i$ rises. *P<0.05 vs. Ca^{2+}-free. p-, para.

to the same concentration of the solvent (without p-cresol or other treatments).

$[Ca^{2+}]_i$ measurement. The cells were grown to 80-90% confluence on 6 cm dishes, trypsinized, and suspended in Ca^{2+}-containing or free medium at a concentration of $1x10^6$ cells/ml. The seeding density for subsequent experiments was $1x10^5$ cells/well in 24-well plates or $5x10^5$ cells/well in 6-well plates. Following addition of 2 μM fura-2-AM for 30 min at 25˚C, cells were washed twice with Ca^{2+}-containing medium before being suspended in Ca^{2+}-containing medium at a concentration of $1x10^7$ cells/ml. Fura-2-AM fluorescence measurements were performed in a water-jacketed cuvette at 25˚C. The cuvette contained 1 ml medium and $5x10^5$ cells. The fluorescence was monitored with a Shimadzu RF-5301PC spectrofluorophotometer. For calibration of $[Ca^{2+}]_i$, Triton X-100 (0.1%) and $CaCl_2$ (5 mM) were added to obtain the maximal fura-2 fluorescence. Ca^{2+} chelator EGTA (10 mM) was added to chelate Ca^{2+} to obtain the minimal fura-2 fluorescence. The fura-2-loaded cells were excited alternately at 340 and 380 nm and emission was recorded at 510 nm. The fluorescence ratio (F340/F380) was used to estimate $[Ca^{2+}]_i$. The fluorescence ratio was calibrated using standard solutions with known Ca^{2+} concentrations and ionophore treatments to determine minimum and maximum fluorescence ratios (23). EC_{50} (half-maximal effective concentration) was calculated. Hill equation was used to describe dose-response relationships.

SKF96365 (5 μM) and 2-APB (20 μM), store-operated Ca^{2+} entry modulators, and GF109203X (2 μM), a PKC inhibitor, were applied at 37˚C throughout the experiment assessing p-cresol-induced changes in $[Ca^{2+}]_i$. Nifedipine, a voltage-gated Ca^{2+} channel blocker, was used at a concentration of 10 μM, Thapsigargin (1 μM), ATP (10 μM) as a PLC agonist, U73122 (2 μM) as a PLC inhibitor, and U73343 (2 μM), an inactive analog of U73122, were all included in the experiments to evaluate their effects on intracellular Ca^{2+} dynamics. All treatments were conducted at a temperature of 37˚C and the duration of each treatment was 30 sec.

Mn^{2+} measurement. The experiment involved quenching of fura-2 fluorescence by Mn^{2+} in medium containing Ca^{2+} and 50 μM $MnCl_2$. $MnCl_2$ was added to the cell suspension in the cuvette 30 sec before fluorescence recording. Data was recorded at an excitation signal of 360 nm (Ca^{2+}-insensitive) and an emission signal of 510 nm at 1-sec intervals, as previously described (24).

Cell viability assay. Cell viability assay was conducted following the manufacturer's instructions. Following treatment with p-cresol at 50, 100, 150, 200 and 250 μM at 37˚C for 24 h, WST-1 (10 μM) was added and cells were incubated at 37˚C for 30 min. Cells were treated with 5 μM BAPTA-AM for 1 h at 37˚C before incubating with p-cresol. The absorbance was determined using an ELISA reader at a wavelength of 450 nm, with a reference wavelength of 620 nm for background correction. In the control, cells treated with the vehicle (organic solvent at ≤0.1%) without p-cresol or BAPTA-AM were used as the baseline for normalization.

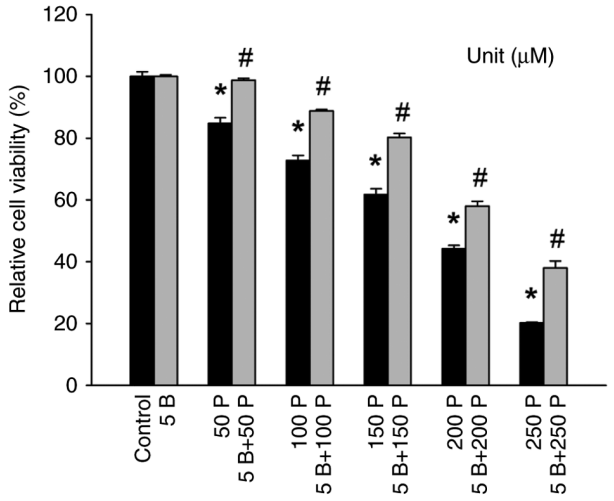

Figure 2. Effect of P on cell viability. *P<0.05 vs. control. #P<0.05 vs. B. P, para-cresol; B, BAPTA-AM.

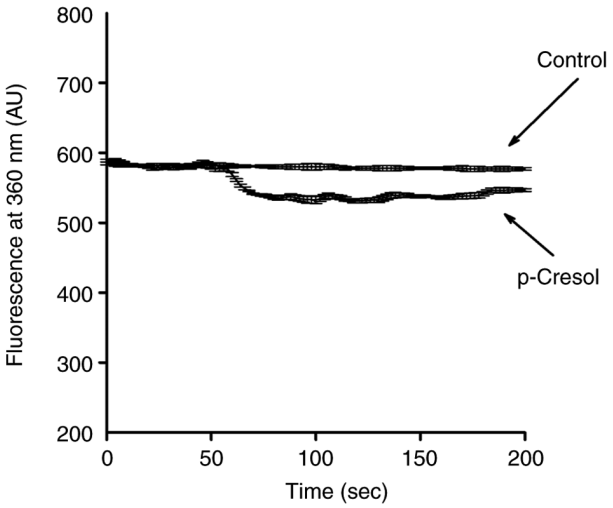

Figure 3. Effect of p-cresol on Ca^{2+} influx using Mn^{2+} quenching of fura-2 fluorescence. $MnCl_2$ (50 μM) was added at 60 sec. p-, para.

Statistical analysis. Data were analyzed using GraphPad Prism version 9.0 (GraphPad Software, Inc.; Dotmatics). Statistical significance was determined using one-way ANOVA followed by Tukey's multiple comparison post hoc test. Tests for normality (Shapiro-Wilk test) and homogeneity of variances (Levene's test) were performed to ensure the assumptions of ANOVA were met. Data are presented as the mean ± SD of three independent experiments. P<0.05 was considered to indicate a statistically significant difference.

Results

p-Cresol increases $[Ca^{2+}]_i$. In Ca^{2+}-containing and -free medium, p-cresol at concentrations between 50 and 150 μM increased $[Ca^{2+}]_i$ in a concentration-dependent manner (Fig. 1B and C). The cells were found to have a viability >95% after 20 min. The cell viability of >95% was determined using the trypan blue exclusion assay. Control experiments confirmed that the organic solvent at a concentration ≤0.1% did not impact cell viability or basal $[Ca^{2+}]_i$ (data not shown). EC_{50} value was 70±2 in a Ca^{2+}-containing and 70±3 μM in Ca^{2+}-free medium by fitting to a Hill equation (Fig. 1D).

Effect of BAPTA-AM on reversing p-cresol-induced cell death. Following exposure of DBTRG-05MG cells to p-cresol, a significant and long-lasting increase in $[Ca^{2+}]_i$ was observed (Fig. 1). Since unregulated $[Ca^{2+}]_i$ can impact cell viability (9,10), the effect of p-cresol on cell viability was investigated. There was a decrease in cell viability in the presence of 50-250 μM p-cresol (Fig. 2). The intracellular Ca^{2+} chelator BAPTA-AM (25) was used to prevent $[Ca^{2+}]_i$ increases during p-cresol treatment. Treatment with 5 μM BAPTA-AM effectively prevented increases in cytosolic Ca^{2+} levels induced by 50-150 μM p-cresol, indicating successful chelation of intracellular Ca^{2+}. Additionally, 5 μM BAPTA-AM did not alter the baseline cell viability, demonstrating its specific action on Ca^{2+} signaling without affecting overall cell health. BAPTA-AM reversed p-cresol-induced decreases in cell viability (Fig. 2).

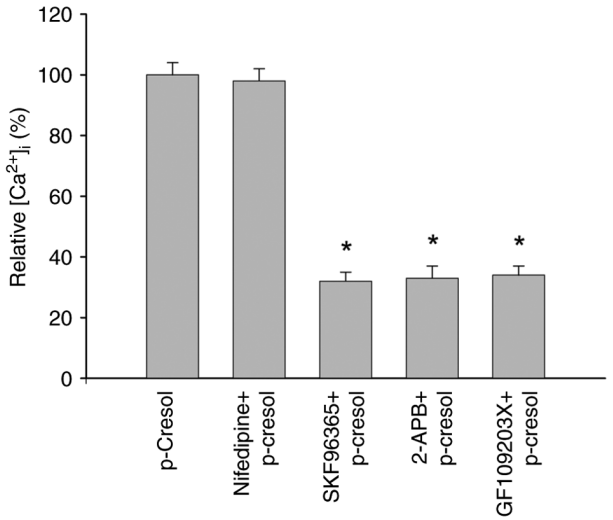

Figure 4. Effect of Ca^{2+} channel modulators on p-cresol-induced $[Ca^{2+}]_i$ rises. *P<0.05 vs. p-cresol. p-, para; 2-APB, 2-aminoethoxydiphenyl borate.

p-Cresol induces Mn^{2+} influx. Experiments were conducted to confirm that increases in $[Ca^{2+}]_i$ in response to p-cresol involved influx of Ca^{2+}. Mn^{2+} enters cells using mechanisms similar to those of Ca^{2+} but quenches fluorescence of the dye fura-2 at all excitation wavelengths (24). Therefore, quenching of fura-2 fluorescence when excited at the Ca^{2+}-insensitive excitation wavelength of 360 nm by Mn^{2+} suggests involvement of Ca^{2+} influx. As the Ca^{2+} response induced by p-cresol peaked at 150 μM, subsequent experiments used 150 μM p-cresol as a control; 150 μM p-cresol triggered an immediate decrease in the 360 nm excitation signal, reaching a maximum value of 62±2 arbitrary units at 100 sec (Fig. 3). This indicated participation of Ca^{2+} influx in p-cresol-induced increases in $[Ca^{2+}]_i$.

Pathways of p-cresol-induced Ca^{2+} entry. Experiments were carried out to investigate the Ca^{2+} entry pathway underlying the p-cresol-induced increases in $[Ca^{2+}]_i$. SKF96365 (5 μM)

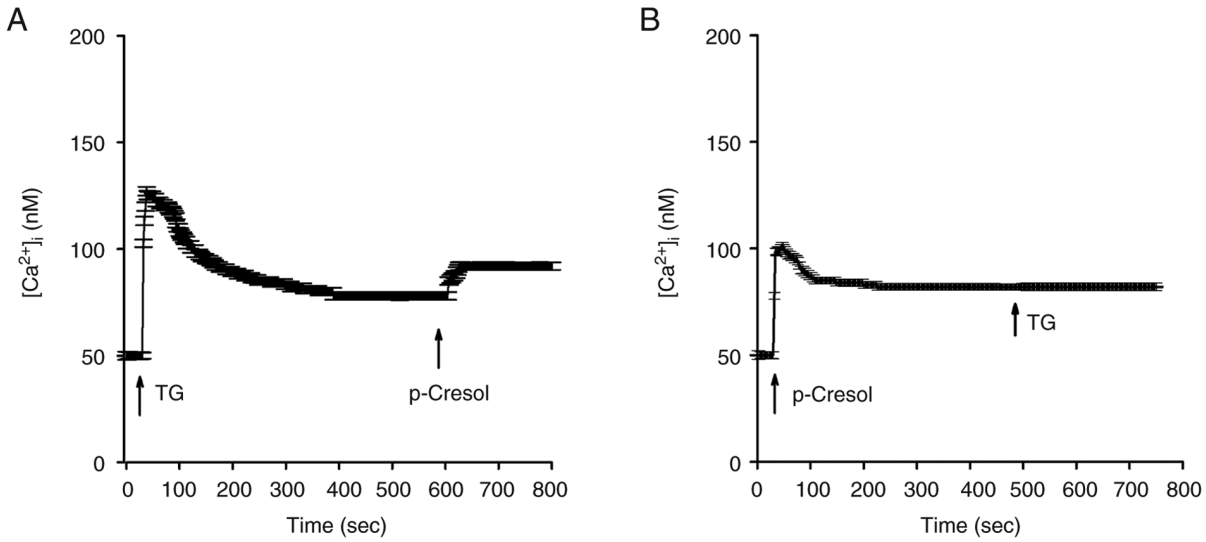

Figure 5. Effect of thapsigargin on p-cresol-induced Ca^{2+} release. (A) 1 μM TG and (B) p-cresol (150 μM) were added. TG, thapsigargin; p-, para.

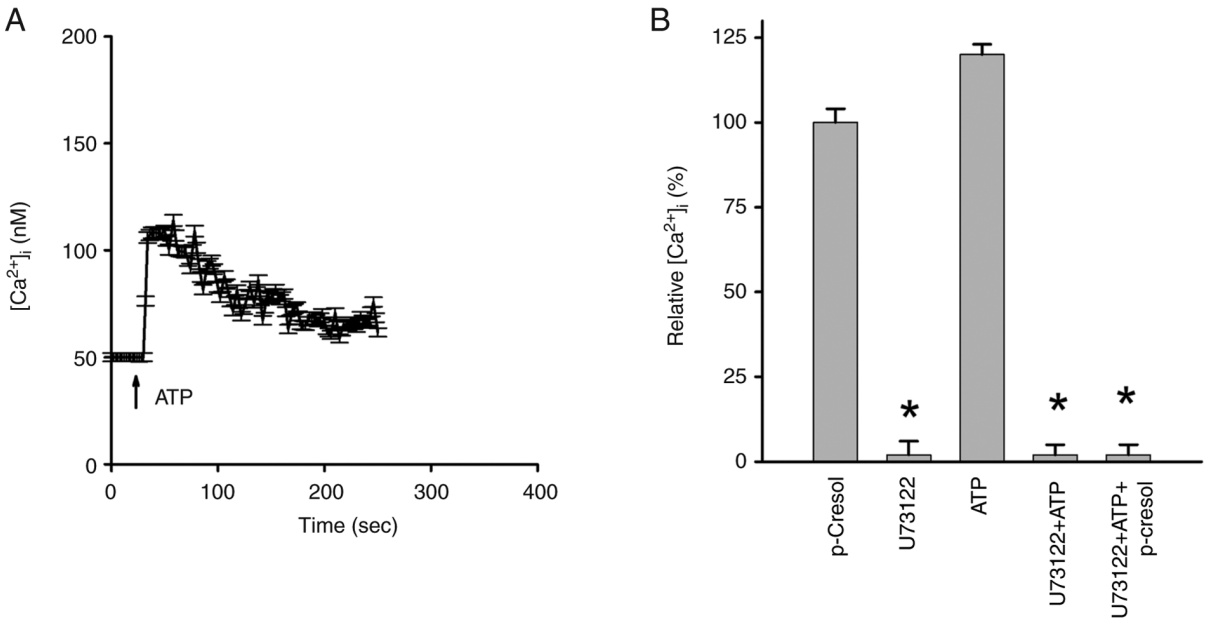

Figure 6. Effect of U73122 on p-cresol-induced Ca^{2+} release. (A) ATP (10 μM) and (B) U73122 (2 μM) and p-cresol (150 μM) were added. *P<0.05 vs. p-cresol. p-, para.

and 2-APB (20 μM), store-operated Ca^{2+} entry modulators (26,27) and GF109203X (2 μM), a PKC inhibitor (28), inhibited p-cresol-induced increases in $[Ca^{2+}]_i$ by 65-70%, but nifedipine (a voltage-gated Ca^{2+} channel blocker, 10 μM) (29) did not (Fig. 4).

Source of p-cresol-induced Ca^{2+} release. The endoplasmic reticulum is the primary Ca^{2+} store in most types of cell, including DBTRG-05MG cells (9,10). Therefore, the present study investigated the role of the endoplasmic reticulum in p-cresol-induced Ca^{2+} release in DBTRG-05MG cells in Ca^{2+}-free medium to eliminate the involvement of Ca^{2+} influx. Addition of 1 μM thapsigargin (30), an inhibitor of the endoplasmic reticulum Ca^{2+} pump, resulted in $[Ca^{2+}]_i$ rises of 75±2 nM (Fig. 5A). Subsequent addition of 150 μM p-cresol induced $[Ca^{2+}]_i$ rises of 10±2 nM. Following p-cresol-induced $[Ca^{2+}]_i$ rises, addition of 1 μM thapsigargin at 500 sec failed to induce further $[Ca^{2+}]_i$ rises (Fig. 5B).

Role of PLC in p-cresol-induced $[Ca^{2+}]_i$ rises. The enzyme PLC serves a key role in regulating release of Ca^{2+} from Ca^{2+} stores (9,10). PLC inhibitor U73122 (31) was applied to investigate if activation of this enzyme was necessary for p-cresol-induced Ca^{2+} release. ATP induced $[Ca^{2+}]_i$ rise of 55±2 nM (Fig. 6A). Since ATP is a PLC-dependent agonist that induces $[Ca^{2+}]_i$ rises in most types of cell (32), it was used to study the inhibitory effect of U73122 on PLC activity. Incubation with 2 μM U73122 did not affect basal $[Ca^{2+}]_i$ but eliminated ATP-induced $[Ca^{2+}]_i$ rises, suggesting effective suppression of PLC activity (Fig. 6B). Additionally, incubation with 2 μM U73122 did not alter basal

$[Ca^{2+}]_i$ but abolished 150 μM p-cresol-induced $[Ca^{2+}]_i$ rises. However, U73343 (negative control), an analog of U73122, did not cause inhibition (data not shown).

Discussion

Ca^{2+} signaling is key in regulating physiological processes in human cells, including glioblastoma cells (9,10). Previous studies have shown that the cresol-related compound 4-chloro-m-cresol affects Ca^{2+} homeostasis in different cell models, such as human neutrophils (13) and mouse skeletal muscle (14). To the best of our knowledge, however, the present study is the first to demonstrate that p-cresol causes $[Ca^{2+}]_i$ rises in human glioblastoma cells. p-Cresol between 50 and 150 μM induced a concentration-dependent increase in $[Ca^{2+}]_i$. The mechanism underlying this increase may involve depleting intracellular Ca^{2+} stores and causing Ca^{2+} influx from the extracellular environment. p-Cresol-induced $[Ca^{2+}]_i$ rises are significantly reduced in the absence of extracellular Ca^{2+}, which suggests that Ca^{2+} influx occurred continuously throughout the stimulation period. This indicates that p-cresol triggers Ca^{2+} influx from extracellular sources, likely through mechanisms such as store-operated Ca^{2+} entry or other channels sensitive to changes in membrane potential or receptor activation.

p-cresol is toxic to glioblastoma cells. Excessive Ca^{2+} in cells can lead to detrimental changes in cell viability, including apoptosis, necrosis, and impaired cellular functions. These effects occur due to disrupted Ca^{2+} homeostasis, which can activate enzymes like proteases and phosphatases, destabilize mitochondrial function, and induce oxidative stress, ultimately contributing to cell death or dysfunction (9,10). Ca^{2+} mobilization causes Ca^{2+} influx across the plasma membrane via store-operated Ca^{2+} entry (9,10). If elevation in $[Ca^{2+}]_i$ is prolonged, or regulation of $[Ca^{2+}]_i$ is abnormal, it can lead to cell death. The present data suggest that p-cresol-induced cell death depended on the rise in $[Ca^{2+}]_i$. Furthermore, increased $[Ca^{2+}]_i$ levels may affect Ca^{2+}-dependent downstream responses, leading to changes in cell physiology (for example, activation of calmodulin-dependent enzymes, modulation of ion channel activity, regulation of gene expression through Ca^{2+}-responsive transcription factors like NFAT (nuclear factor of activated T-cells), and triggering of apoptotic pathways via activation of caspases (9,10). These responses highlight the critical role of Ca^{2+} signaling in regulating cellular processes such as metabolism, proliferation, and cell fate determination (9,10).

p-Cresol causes entry of Ca^{2+} by stimulating store-operated Ca^{2+} entry. The depletion of intracellular Ca^{2+} stores induces this entry (9,10). p-cresol-induced $[Ca^{2+}]_i$ rises were inhibited by specific compounds, namely SKF96365 and 2-APB, which are often used as modulators of store-operated Ca^{2+} entry in various types of cell, such as cortical neurons, myofibroblasts, T lymphocytes, and rat sensory neurons (26,27,33,34). The present data showed that these modulators inhibited p-cresol-induced $[Ca^{2+}]_i$ rises. On the other hand, nifedipine, a voltage-gated Ca^{2+} channel blocker (20), did not inhibit p-cresol-induced $[Ca^{2+}]_i$ rises, which suggested that p-cresol-induced Ca^{2+} entry occurred via a store-operated Ca^{2+} pathway.

Ca^{2+} stores in thapsigargin-sensitive endoplasmic reticulum serve a dominant role in p-cresol-induced Ca^{2+} release. PLC produces IP_3 and DAG when activated, activating PKC (9,10). To examine the effect of modulation of PKC activity on p-cresol-induced $[Ca^{2+}]_i$ rises, PKC inhibitor GF109203X was used. PKC is involved in signaling pathways that regulate Ca^{2+} dynamics; inhibiting PKC with GF109203X attenuated or blocked the increase in $[Ca^{2+}]_i$ typically triggered by p-cresol Additionally, the release of Ca^{2+} was PLC-dependent, as shown by the abolition of release when PLC activity was decreased by the inhibitor U73122.

The present results showed a significant increase in $[Ca^{2+}]_i$ following p-cresol treatment. This suggested that p-cresol disrupted Ca^{2+} homeostasis, potentially by enhancing Ca^{2+} influx or inhibiting Ca^{2+} efflux mechanisms. The increase in Ca^{2+} levels may be attributed to the activation of store-operated Ca^{2+} entry channels or inhibition of Ca^{2+}-ATPases on the endoplasmic reticulum (9,10). There was a dose-dependent decrease in cell viability with p-cresol treatment, which aligned with disruptions in Ca^{2+} signaling. Dysregulated Ca^{2+} signaling can lead to mitochondrial dysfunction, triggering cell death pathways (9,10). The decrease in cell viability supports this mechanistic pathway, where p-cresol-induced Ca^{2+} dysregulation results in cell death. The present results provide more robust and comprehensive understanding of how p-cresol affects Ca^{2+} signaling in glioma cells.

Exposing cells to 100 μM p-cresol for 24 h can induce cell death due to its cytotoxic effects. This concentration exceeds physiological levels typically found in plasma, which are 20-40 μM for cresol compounds *in vivo* (8,35). Elevated plasma levels of cresol compounds, especially in patients with liver or kidney disorders (8,35), may further increase the concentration of p-cresol beyond normal physiological ranges, exacerbating its cytotoxic effects. Although the present study does not focus on liver or kidney disorders, this information is relevant to understanding the potential cytotoxicity and biological effects of p-cresol at concentrations that may exceed physiological levels observed in healthy individuals. This broader context helps interpret the impact of p-cresol on cellular systems and provides insights into its potential health implications under different physiological conditions. The potential use of p-cresol or its derivatives in treating human glioblastoma requires further exploration. The effect of p-cresol should be studied *in vivo*. Furthermore, since increases in $[Ca^{2+}]_i$ levels affect numerous Ca^{2+}-coupled cellular processes, these include activation of calmodulin-dependent enzymes involved in signal transduction, modulation of ion channel activity influencing membrane potential and neurotransmitter release, and initiation of apoptotic pathways through activation of caspases, highlighting the pivotal role of Ca^{2+} signaling in regulating diverse cellular functions (9,10). The effect of p-cresol-induced $[Ca^{2+}]_i$ rises on other cellular responses requires further exploration.

The present study had a limited sample size, which may decrease statistical power and generalizability. A small sample size increases risk of errors, potentially overlooking subtle but biologically significant effects of p-cresol. Future studies should increase the sample size to validate the present findings. Furthermore, the present study utilized *in vitro* models (human

glioblastoma cell line) to investigate the effects of p-cresol. *In vitro* models do not fully replicate the complexity of *in vivo* tumor microenvironments, such as presence of immune cells, extracellular matrix components and dynamic interactions with other types of cell. While the present study primarily addressed the short-term impacts, it is necessary to understand how p-cresol influences cell behavior over extended periods. Additional experiments should assess long-term effects of p-cresol on glioblastoma cell survival and proliferation.

Proteomic and transcriptomic analyses should be performed to uncover the precise molecular targets of p-cresol. Mass spectrometry-based proteomics can identify protein modifications and changes in expression in response to p-cresol treatment. RNA sequencing can reveal gene expression and signaling pathway alterations. Understanding the specific molecular pathways p-cresol affects may identify novel therapeutic targets for glioblastoma treatment. Furthermore, long-term exposure studies using glioblastoma xenograft models in immunocompromised mice are required. These studies may provide insight into the chronic effects of p-cresol and its potential as a therapeutic agent *in vivo*, as well as assess the safety and efficacy of p-cresol in a more physiologically relevant context. Future research should determine the detailed mechanism of p-cresol, explore its long-term effects *in vivo*, investigate combination therapies with existing chemotherapeutic agents or targeted therapies, expand its application to other types of cancer, and develop optimized derivatives to advance understanding and therapeutic potential of p-cresol in cancer treatment.

Phosphoproteomics analysis should be performed to identify signaling pathways activated downstream of Ca^{2+} influx in response to p-cresol treatment. This approach maps phosphorylation changes in proteins involved in key signaling pathways. Glioblastoma cells treated with p-cresol should be analyzed using mass spectrometry-based phosphoproteomics to identify differentially phosphorylated proteins. Bioinformatics tools should be used to map these proteins to specific signaling pathways. To provide a more holistic view of the biological effects of p-cresol, additional experiments to assess its impact on oxidative stress, autophagy, and mitochondrial function should be performed to provide insights into the mechanisms underlying its cytotoxic effects and uncover potential therapeutic targets for glioblastoma treatment.

PLC serves a key role is in p-cresol-induced Ca^{2+} signaling. To investigate the involvement of specific PLC isoforms in p-cresol-induced Ca^{2+} release in glioblastoma cells, molecular biology techniques such as gene expression analysis and siRNA-mediated knockdown will be employed. These methods aim to determine the expression levels and functional significance of different PLC isoforms when glioblastoma cells are treated with p-cresol. Identifying the PLC family and specific isoform(s) involved will provide insights into the molecular mechanisms underlying the dysregulation of p-cresol-induced Ca^{2+} signaling. Additionally, the functional role of the identified PLC isoforms in p-cresol-induced Ca^{2+} release and its downstream effects on glioblastoma cell physiology will be assessed. This will involve using pharmacological inhibitors or activators specific to the identified PLC isoform(s) to modulate its activity. The impact on intracellular Ca^{2+} dynamics, as well as on cell viability, proliferation, and migration, will be evaluated to understand the broader implications of PLC-mediated signaling pathways in p-cresol-treated glioblastoma cells. Functional analysis may elucidate the contribution of PLC isoform(s) to p-cresol-induced Ca^{2+} signaling alterations and provide mechanistic insights into glioblastoma pathophysiology. This may determine involvement of specific PLC isoforms in p-cresol-induced Ca^{2+} release and elucidate their functional role in glioblastoma cells. These investigations may provide valuable insight into the molecular mechanisms underlying Ca^{2+} signaling dysregulation in glioblastoma and uncover novel therapeutic targets for glioblastoma treatment.

In conclusion, p-cresol induced Ca^{2+} entry in DBTRG-05MG human glioblastoma cells via a PKC-dependent, store-operated mechanism. p-Cresol triggered release of Ca^{2+} from the endoplasmic reticulum via a PLC-dependent pathway. This led to cell death, which is initiated by a Ca^{2+} signal. The impact of p-cresol on Ca^{2+} movement in glioblastoma cells should be investigated *in vitro* and *in vivo*.

Acknowledgements

Not applicable.

Funding

The present study was supported by Department of Pharmacy and Master Program, College of Pharmacy and Health Care, Tajen University.

Availability of data and materials

The data generated in the present study may be requested from the corresponding author.

Authors' contributions

PHC, CLS, SHF, RS and WZL all contributed substantially to the conception and design, acquisition of data, or analysis and interpretation of data. PHC, CLS, SHF and RS confirm the authenticity of all the raw data. WZL wrote the manuscript. All authors have read and approved the final manuscript.

Ethics approval and consent to participate

Not applicable.

Patient consent for publication

Not applicable.

Competing interests

The authors declare that they have no competing interests.

References

1. Aranha MM, Matos AR, Teresa Mendes A, Vaz Pinto V, Rodrigues CM and Arrabaça JD: Dinitro-o-cresol induces apoptosis-like cell death but not alternative oxidase expression in soybean cells. J Plant Physiol 164: 675-684, 2007.

2. Mariot P, Prevarskaya N, Roudbaraki MM, Le Bourhis X, Van Coppenolle F, Vanoverberghe K and Skryma R: Evidence of functional ryanodine receptor involved in apoptosis of prostate cancer (LNCaP) cells. Prostate 43: 205-214, 2000.
3. Yue Z, She RP, Bao HH, Tian J, Yu P, Zhu J, Chang L, Ding Y and Sun Q: Necrosis and apoptosis of renal tubular epithelial cells in rats exposed to 3-methyl-4-nitrophenol. Environ Toxicol 27: 653-661, 2012.
4. Hsu JE, Lo SH, Lin YY, Wang HT and Chen CY: Effects of essential oil mixtures on nitrogen metabolism and odor emission via in vitro simulated digestion and in vivo growing pig experiments. J Sci Food Agric 102: 1939-1947, 2022.
5. Saleh-E-In MM, Bhattacharyya P and Van Staden J: Chemical composition and cytotoxic activity of the essential oil and oleoresins of in vitro micropropagated Ansellia africana Lindl: A Vulnerable Medicinal Orchid of Africa. Molecules 26: 4556, 2021.
6. Tanaka S, Yano S, Sheikh AM, Nagai A and Sugimoto T: Effects of uremic toxin p-cresol on proliferation, apoptosis, differentiation, and glucose uptake in 3T3-L1 cells. Artif Organs 38: 566-571, 2014.
7. de Carvalho JT Jr, Dalboni MA, Watanabe R, Peres AT, Goes MA, Manfredi SR, Canziani ME, Cendoroglo GS, Guimaraes-Souza N, Batista MC and Cendoroglo M: Effects of spermidine and p-cresol on polymorphonuclear cell apoptosis and function. Artif Organs 35: E27-E32, 2011.
8. Letertre MPM, Myridakis A, Whiley L, Camuzeaux S, Lewis MR, Chappell KE, Thaikkatil A, Dumas ME, Nicholson JK, Swann JR and Wilson ID: A targeted ultra performance liquid chromatography-Tandem mass spectrometric assay for tyrosine and metabolites in urine and plasma: Application to the effects of antibiotics on mice. J Chromatogr B Analyt Technol Biomed Life Sci 1164: 122511, 2021.
9. Berridge MJ: Calcium signalling in health and disease. Biochem Biophys Res Commun 485: 5, 2017.
10. Bootman MD and Bultynck G: Fundamentals of cellular calcium signaling: A Primer. Cold Spring Harb Perspect Biol 12: a038802, 2020.
11. Al-Mousa F and Michelangeli F: Commonly used ryanodine receptor activator, 4-chloro-m-cresol(4CmC), is also an inhibitor of SERCA Ca^{2+} pumps. Pharmacol Rep 61: 838-842, 2009.
12. Lin AH, Sun H, Paudel O, Lin MJ and Sham JS: Conformation of ryanodine receptor-2 gates store-operated calcium entry in rat pulmonary arterial myocytes. Cardiovasc Res 111: 94-104, 2016.
13. Hauser CJ, Kannan KB, Deitch EA and Itagaki K: Non-specific effects of 4-chloro-m-cresol may cause calcium flux and respiratory burst in human neutrophils. Biochem Biophys Res Commun 336: 1087-1095, 2005.
14. Arai S, Ikeda M, Ide T, Matsuo Y, Fujino T, Hirano K, Sunagawa K and Tsutsui H: Functional loss of DHRS7C induces intracellular Ca^{2+} overload and myotube enlargement in C2C12 cells via calpain activation. Am J Physiol Cell Physiol 312: C29-C39, 2017.
15. Suzuki D, Hori T, Saitoh N and Takahashi T: 4-Chloro-m-cresol, an activator of ryanodine receptors, inhibits voltage-gated K^+ channels at the rat calyx of Held. Eur J Neurosci 26: 1530-1536, 2007.
16. Baqri W, Rzadki K, Habbous S and Das S: Treatment, healthcare utilization and outcomes in patients with glioblastoma in Ontario: A 10-year cohort study. J Neurooncol 168: 473-485, 2024.
17. Liang T, Gu L, Kang X, Li J, Song Y, Wang Y and Ma W: Programmed cell death disrupts inflammatory tumor microenvironment (TME) and promotes glioblastoma evolution. Cell Commun Signal 22: 333, 2024.
18. Srivastava R, Dodda M, Zou H, Li X and Hu B: Tumor Niches: Perspectives for targeted therapies in glioblastoma. Antioxid Redox Signal 39: 904-922, 2023.
19. Stachulski AV, Knausenberger TB, Shah SN, Hoyles L and McArthur S: A host-gut microbial amino acid co-metabolite, p-cresol glucuronide, promotes blood-brain barrier integrity in vivo. Tissue Barriers 11: 2073175, 2023.
20. Chang KF, Liu CY, Huang YC, Hsiao CY and Tsai NM: Downregulation of VEGFR2 signaling by cedrol abrogates VEGF-driven angiogenesis and proliferation of glioblastoma cells through AKT/P70S6K and MAPK/ERK1/2 pathways. Oncol Lett 26: 342, 2023.
21. Ertilav K and Nazıroğlu M: Honeybee venom melittin increases the oxidant activity of cisplatin and kills human glioblastoma cells by stimulating the TRPM2 channel. Toxicon 222: 106993, 2023.
22. Akyuva Y and Nazıroğlu M: Silver nanoparticles potentiate antitumor and oxidant actions of cisplatin via the stimulation of TRPM2 channel in glioblastoma tumor cells. Chem Biol Interact 369: 110261, 2023.
23. Ashokan A and Aradhyam GK: Measurement of intracellular Ca^{2+} mobilization to study GPCR signal transduction. Methods Cell Biol 142: 59-66, 2017.
24. Absi M, Eid BG, Ashton N, Hart G and Gurney AM: Simvastatin causes pulmonary artery relaxation by blocking smooth muscle ROCK and calcium channels: Evidence for an endothelium-independent mechanism. PLoS One 14: e0220473, 2019.
25. Segal S and Yaniv Y: Ca^{2+}-Driven selectivity of the effect of the cardiotonic steroid marinobufagenin on rabbit sinoatrial node function. Cells 12: 1881, 2023.
26. Gruszczynska-Biegala J, Strucinska K, Maciag F, Majewski L, Sladowska M and Kuznicki J: STIM Protein-NMDA2 receptor interaction decreases NMDA-Dependent calcium levels in cortical neurons. Cells 9: 160, 2020.
27. Hsu WL, Hsieh YC, Yu HS, Yoshioka T and Wu CY: 2-Aminoethyl diphenylborinate inhibits bleomycin-induced skin and pulmonary fibrosis via interrupting intracellular Ca^{2+} regulation. J Dermatol Sci 103: 101-108, 2021.
28. Chiu KM, Lee MY, Lu CW, Lin TY and Wang SJ: Plantainoside D reduces depolarization-evoked glutamate release from rat cerebral cortical synaptosomes. Molecules 28: 1313, 2023.
29. Tauskela JS, Brunette E, Aylsworth A and Zhao X: Neuroprotection against supra-lethal 'stroke in a dish' insults by an anti-excitotoxic receptor antagonist cocktail. Neurochem Int 158: 105381, 2022.
30. Couly S, Yasui Y, Foncham S, Grammatikakis I, Lal A, Shi L and Su TP: Benzomorphan and non-benzomorphan agonists differentially alter sigma-1 receptor quaternary structure, as does types of cellular stress. Cell Mol Life Sci 81: 14, 2024.
31. Hung Y, Chung CC, Chen YC, Kao YH, Lin WS, Chen SA and Chen YJ: Klotho modulates pro-fibrotic activities in human atrial fibroblasts through inhibition of phospholipase C signaling and suppression of store-operated calcium entry. Biomedicines 10: 1574, 2022.
32. Liu Z, Wu X, Wang Q, Li Z, Liu X, Sheng X, Zhu H, Zhang M, Xu J, Feng X, *et al*: CD73-Adenosine A1R Axis regulates the activation and apoptosis of hepatic stellate cells through the PLC-IP3-Ca^{2+}/DAG-PKC signaling pathway. Front Pharmacol 13: 922885, 2022.
33. Ishikawa J, Ohga K, Yoshino T, Takezawa R, Ichikawa A, Kubota H and Yamada T: A pyrazole derivative, YM-58483, potently inhibits store-operated sustained Ca^{2+} influx and IL-2 production in T lymphocytes. J Immunol 170: 4441-4449, 2003.
34. Shideman CR, Reinardy JL and Thayer SA: gamma-Secretase activity modulates store-operated Ca^{2+} entry into rat sensory neurons. Neurosci Lett 451: 124-128, 2009.
35. Cuoghi A, Caiazzo M, Bellei E, Monari E, Bergamini S, Palladino G, Ozben T and Tomasi A: Quantification of p-cresol sulphate in human plasma by selected reaction monitoring. Anal Bioanal Chem 404: 2097-2104, 2012.